Effect of Functional Groups at Hole Edges on Cisplatin Release from Inside Single-Wall Carbon Nanohorns

Kumiko Ajima,* Masako Yudasaka, Alan Maigné, Jin Miyawaki, and Sumio Iijima

JST/SORST, NEC Fundamental Laboratories, 34 Miyukigaoka, Tsukuba 305-8501, Japan

Received: November 24, 2005; In Final Form: January 18, 2006

We incorporated cisplatin inside single-wall carbon nanohorns (NHs) and revealed that 70% of the cisplatin was released from NHs having holes with hydrogen-terminated edges when they were immersed in phosphate-buffered saline (PBS). However, only 15% was released from NHs having holes with oxygen-containing functional groups at the hole edges (NHox). Elemental analysis indicated that −COOH and −OH groups at the hole edges of NHox changed mainly to −COONa and −ONa groups by immersion in PBS. These groups decreased the practical hole diameters, which resulted in hindering the cisplatin release from NHox. This means that the release of the material from inside NHox would be controlled by chemically modifying the functional groups attached to the hole edges of NHox; thus the potential applicability of NHox to a material carrier would be enhanced.

Introduction

The targeted delivery of cisplatin (CDDP, $(NH_3)_2PtCl_2$), an anticancer drug, has been well investigated in vitro and in vivo for cancer chemotherapy. Macromolecule carrier systems can selectively deliver cisplatin to tumors through the enhanced permeability and retention effect.[1] Cisplatin−macromolecule systems have already been used to effectively suppress in vivo tumor growth; [2−6] moreover, studies of delivery systems using liposomes,[7] gelatin hydrogel,[2] and polymer micelles[8] have revealed that the nephrotoxicity side effect of cisplatin is reduced in rats and mice.

The effective delivery of cisplatin requires controlled release. Release from polymeric micelles is controlled by modulating the decay properties of the polymeric micelles.[9] The biodegradation of various microcarriers produces a sustained release in vitro[10,11] and in vivo.[2]

The nanometer scale of carbon nanotubes (CNTs)[12,13] makes them well suited for carrying biomolecules such as DNA and proteins.[14−16] Their chemical and mechanical stability ensures their transportation without degradation in the human body. Chemical modifications of CNTs should give them a targeting ability and enhance their biocompatibility. Moreover, the nanospaces in CNTs are suitable for encapsulating drugs.

We have been studying the use of single-wall carbon nanohorns (NHs),[17] a type of single-wall CNT,[13] as drug carriers. Dexamethasone, an antiinflammatory drug, was shown to be adsorbed by NHs, and the released dexamethasone retained its effects in vitro.[18] More recently, cisplatin was also shown to be incorporated in NHs, and the released cisplatin retained its ability to kill human cancer cells in a cell culture medium.[19] NHs have several advantages over single-wall CNTs for drug delivery systems. The holes are easily opened on the NH walls by heat treatment in O_2 gas,[20] the number and size of the holes can be changed by controlling the heat-treatment conditions,[21] and the inside spaces are sufficiently wide for the large molecules to be incorporated. NHs with opened holes are thus well suited for drug incorporation and controlled release.

* Author to whom correspondence should be addressed. E-mail: kumikoajima@frl.cl.nec.co.jp.

However, several issues must be addressed before NHs can be used as practical carriers of drugs and genes. One issue is the effect of the hole-edge structure on drug incorporation and release. We have investigated this effect by comparing the incorporation and release abilities of NHs having holes with oxygen-containing functional groups at the hole edges (NHox) and NHs having holes with hydrogen-terminated edges (NHh).

Experimental Section

We prepared NHs by CO_2 laser ablation of graphite in Ar (760 Torr) at room temperature.[17] The NHox was obtained by treating NHs in flowing O_2 gas at 570−580 °C for 10 min.[19] The NHh was obtained by removing the oxygen-containing functional groups from the hole edges by treating NHox in flowing H_2 gas at 1200 °C for 3 h.[22]

CDDP was incorporated in the NHox and NHh using the nanoprecipitation method.[19,23] CDDP was dissolved in dimethylformamide (DMF) to a concentration of 4.15 mg mL^{-1}. NHox or NHh (50 mg) was mixed in the CDDP−DMF solution (10 mL) in a beaker, and the mixture was left in the beaker in flowing dry air until the DMF evaporated. The obtained powders were observed with a high-resolution transmission electron microscope (HRTEM) and a scanning transmission electron microscope (STEM) using a high-angle annular dark-field technique (Z-contrast image, Z = atomic number). We refer to the CDDP-incorporated NHox and NHh as "CDDP@NHox" and "CDDP@NHh", respectively. We used CDDP recrystallized from the DMF solution as a control sample.

The quantities of the CDDP in CDDP@NHox and CDDP@NHh were estimated through thermogravimetric analysis (TGA) carried out in O_2 atmosphere from room temperature to 1000 °C with a heating rate of 10 °C min^{-1}. X-ray diffraction (XRD) of CDDP@NHox and CDDP@NHh clarified the sizes of the CDDP crystallites that were deposited outside the NHox.

To estimate the release rate of CDDP from CDDP@NHox and CDDP@NHh in phosphate-buffered saline (PBS), we dispersed CDDP@NHox or CDDP@NHh (CDDP, 1.2 mg) in PBS (2 mL) inside a dialysis-membrane cylinder with 10-kDa pores and immersed the cylinder in PBS (598 mL). As CDDP

10.1021/jp056813x CCC: $33.50
Published on Web 02/24/2006

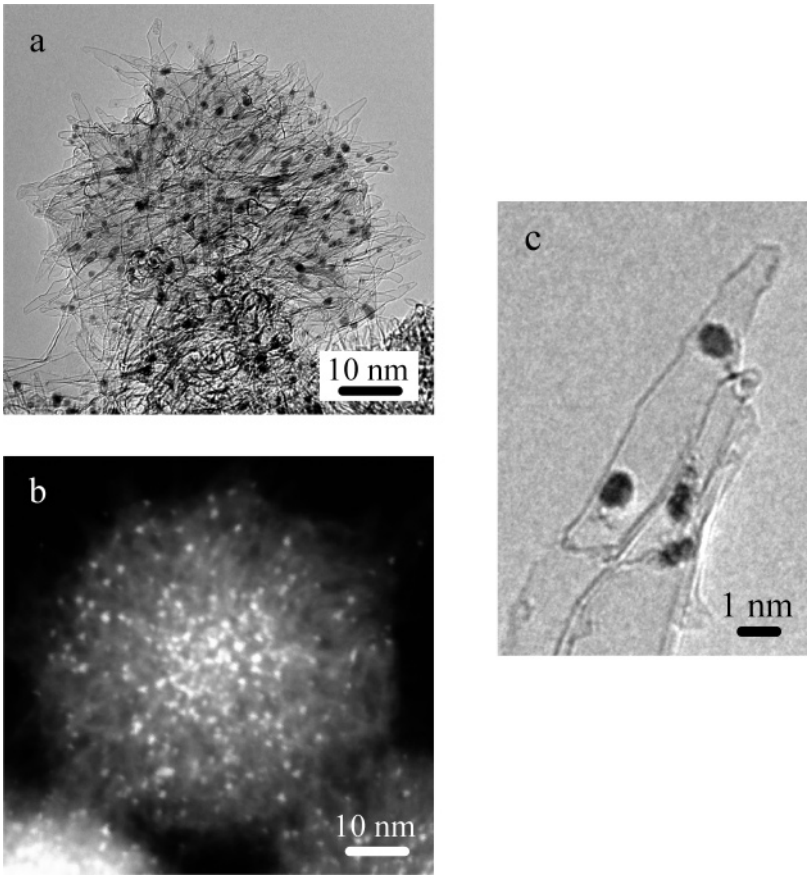

Figure 1. (a) HRTEM micrograph of CDDP@NHox. (b) Z-contrast/STEM micrograph of CDDP@NHox. (c) Magnified HRTEM micrograph of CDDP@NHox.

diffused out of the cylinder, we periodically took 1-mL samples of the CDDP−PBS solution outside the cylinder. From the measured atomic absorption spectra (AAS) of these samples, we estimated the quantity of Pt in each sample, which we then used to estimate the quantity of CDDP released. The release experiment was also carried out in water, and the results obtained were compared with those obtained using PBS.

To investigate the reasons for CDDP release rates and quantities of CDDP@NHh differing from those of CDDP@NHox, we examined the effect of PBS adsorption on NHox and NHh. We dispersed NHox or NHh in PBS solution (1 mg mL^{-1}) and stirred the solution for 1 h. Using a filter paper with a pore size of 200 nm, we filtered 10 mL of the solution and washed the filtered material with 10 mL of water three times to cut PBS solution remaining outside and inside the NHox or NHh. The obtained material was dried in flowing dry air. We referred to these specimens as "PBS−NHox" and "PBS−NHh". TGA was performed to clarify their combustion temperatures, and low-dose energy-dispersive X-ray spectra (XEDS) were observed to quantify the PBS elements (Na, Cl, P, K) absorbed. The XEDS measurements were performed with an HRTEM (002B, Topcon equipped with an X-ray detector (5538A-4SUS-SN, Thermo Electron, Inc.) operated at 120 keV. The peaks were integrated using a digital top-hat filter to remove the background. The *k*-factors used for the quantification were calculated from calibrations with cisplatin crystals, Pt inserted in the single-wall NHs, and PBS crystallites.

Results and Discussion

Structure and Quantities. HRTEM images (Figures 1a and 1c) and a Z-contrast image (Figure 1b) of CDDP@NHox revealed CDDP clusters incorporated in the NHox aggregate, with cluster sizes of about 1−2 nm (Figure 1c), in line with previous results for CDDP@NHh.[19] We did not find any CDDP crystallites existing outside of NHox or NHh in HRTEM observations.

The TGAs of NHox, NHh, and the neat CDDP crystallites were compared with those for CDDP@NHox and CDDP@NHh. The derivative curve of the weight decrease for NHox exhibited a peak at about 635 °C and a shoulder at about 660 °C (Figure 2a). The former corresponds to the combustion of NHox, and the latter corresponds to the combustion of graphitic particles.[24] The derivative curve for NHh exhibited peaks at 635 and 715 °C (Figure 2b), corresponding to the burning of NHh and graphitic particles, respectively. The reason for the lower combustion temperature of the graphitic particles for NHox (Figure 2a) is not clear.

The TGA of CDDP@NHox (Figure 2d) and CDDP@NHh (Figure 2e) indicated that the CDDP quantities were 0.24 and 0.21 g per 1 g of NHox and NHh, respectively (Table 1). The residues at 1000 °C were Pt, and their quantities were 12.3% and 11.4% for CDDP@NHox and CDDP@NHh. From these values, the CDDP quantities were calculated to be 18.9% and 17.6% for CDDP@NHox and CDDP@NHh, respectively. The weight-loss value caused by the combustion of NHox of CDDP@NHox was 79% in a range between 430 and 1000 °C (Figure 2d), and that of NHh of CDDP@NHh was 82% in a range between 400 and 1000 °C (Figure 2e). Note that the quantity of NHox or NHh included that of the graphitic particles. The weight decrease at about 100 °C corresponded to DMF desorption (Figures 2d and 2e). Although degradation of the neat CDDP crystallites was observed at about 330 °C (Figure

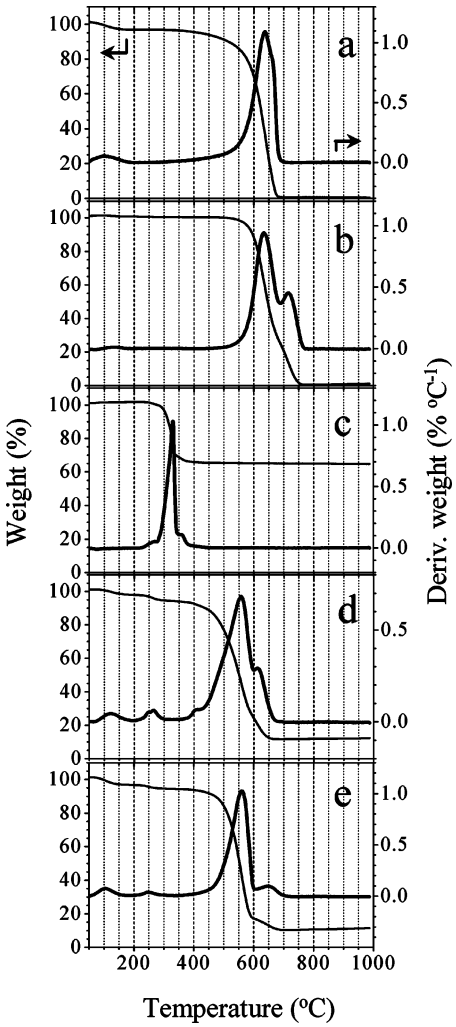

Figure 2. Thermogravimetry (thin lines) and differential thermogravimetry (bold lines) curves of (a) NHox treated with DMF, (b) NHh treated with DMF, (c) CDDP powder treated with DMF, (d) CDDP@NHox, and (e) CDDP@NHh.

2c), the CDDP of CDDP@NHox combusted or degraded at different temperatures, at about 250 and at about 400 °C. For CDDP@NHh, the CDDP combusted or degraded at about 250 °C. The reasons that the combustion/degradation temperatures of the CDDP of CDDP@NHox and CDDP@NHh were lower than those of the CDDP crystallites and that the combustion/degradation temperatures of the CDDP of CDDP@NHox fell into two ranges are not clear. The combustion temperatures of NHox and NHh (Figures 2a and 2b) decreased from 635 to 560 °C when CDDP was incorporated (Figures 2d and 2e). The reason for these decreases in the combustion temperatures was

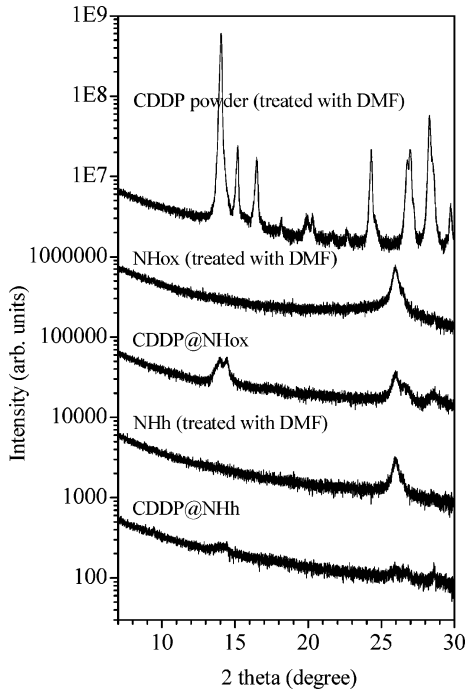

Figure 3. X-ray diffraction patterns.

that the decomposed fragments of Pt functioned as a catalyst for the combustion of NHox and NHh.

XRD patterns of CDDP@NHox and CDDP@NHh showed diffraction peaks characteristic of CDDP at 2θ of about 14° (Figure 3). A rough estimation using the width of the peaks and the Scherrer equation showed that particle sizes were about 20−50 nm, meaning that they likely existed outside NHox and NHh. Since the CDDP crystallites with the sizes of 20−50 nm were not found in HRTEM observations, their quantity must be small. The peaks at about 26.5° (Figure 3) are ascribed to graphitic impurities in the nanohorns.[24] The CDDP clusters with sizes of 1−2 nm inside the nanospaces of NHox (Figure 1) or NHh (not shown)[19] could not exhibit peaks due to their poor crystallinity and/or small crystal sizes. The poor crystallinity and/or small crystal size usually make the XRD peaks too broad to be observed.

The results shown above indicate that there were little differences between CDDP@NHox and CDDP@NHh in structure, quantity of the incorporated CDDP, and size of the CDDP clusters. However, we found that the quantities of CDDP released from CDDP@NHox and CDDP@NHh in PBS were extremely different, which is shown below.

Release of CDDP from NHox and NHh in PBS. We estimated the quantities of CDDP released from CDDP@NHox and CDDP@NHh when they were immersed in PBS by AAS measurements. The results showed that only 15% was released

TABLE 1: Quantities of CDDP Encapsulated in NHox and NHh and Combustion Temperatures of NHox and NHh, as Estimated from TGA[a]

			CDDP@NHox	CDDP@NHh
TGA	quantities of CDDP in NHs (g/g)[b]		0.24	0.21
	combustion temperatures of NHs (°C)		556	560
release-profile analysis	quantities of released and not released CDDP (%)	slowly released (1)[c]	13	66
		quickly released (2)[c]	3	4
		not released	85	30
	release rate (h^{-1})	α(1)[c]	0.18	0.05
		β(2)[c]	4.0	1.1

[a] Results of numerical simulation of release profiles shown in Figure 4 are also listed. [b] Weights were estimated as 100% including graphitic particles. [c] (1) and (2) indicate release from inside and outside, respectively.

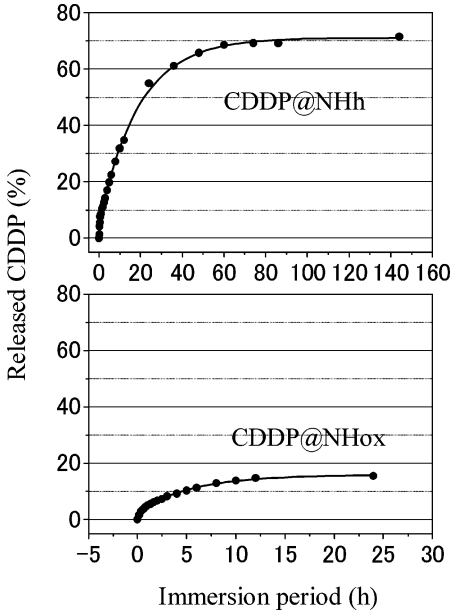

Figure 4. Quantity of CDDP released from CDDP@NHox and CDDP@NHh immersed in PBS versus length of immersion.

from CDDP@NHox, while about 70% was released from the CDDP@NHh (Figure 4).

To investigate the release processes in detail, we first approximate that the release rate was linearly proportional to the CDDP quantity remaining inside NHox or NHh and thus that the release process follows a power law. But with such a model, the first tenth of a minute was not well explained. A better fit was obtained by assuming that two first-order release processes were occurring. Thus we fit the release profile with eq (1) and defined the release rates as the time constants $\alpha(1)$ and $\alpha(2)$

$$N_{\text{released}}(t) = N_0 - N_{\text{not released}} - N_{\text{quiclkly released}}e^{-\alpha(1)t} - N_{\text{slowly released}}e^{-\alpha(2)t} \quad (1)$$

Such primary model well reproduced the experimental release profiles in Figure 4, and a correlation factor superior to 0.998 was obtained in both the cases of NHh and NHox. A more precise model could be too complicated because of the many diffusion processes occurring such as bulk diffusion, surface diffusion, or viscous flow.

The fitting results summarized in Table 1 show that the quantity of the quickly released CDDP from NHox or NHox is small and similar. The CDDP released slowly from both had larger quantities. It should be noted that the CDDP released slowly from CDDP@NHox had a smaller quantity than CDDP@NHh. Taking the results obtained from TEM (Figure 1) observation and XRD measurements (Figure 3) into account, it is concluded that most of the slowly released CDDP was from inside NHox or NHh, while the quickly released CDDP was from those located the outside of NHox or NHh.

Here is an extra explanation on the slow release rates. The slow release of CDDP from the NHh, 0.05 h^{-1} (Table 1), reflects the hydrophobic characteristics of the hydrogen-terminated edges of the holes. We suspect that aqueous solutions cannot easily pass through holes with hydrogen-terminated edges, leading to the slow release of CDDP. Coinciding with this idea, the release rate of CDDP from NHox was higher, 0.18 h^{-1}, than that from NHh, 0.05 h^{-1} (Table 1).

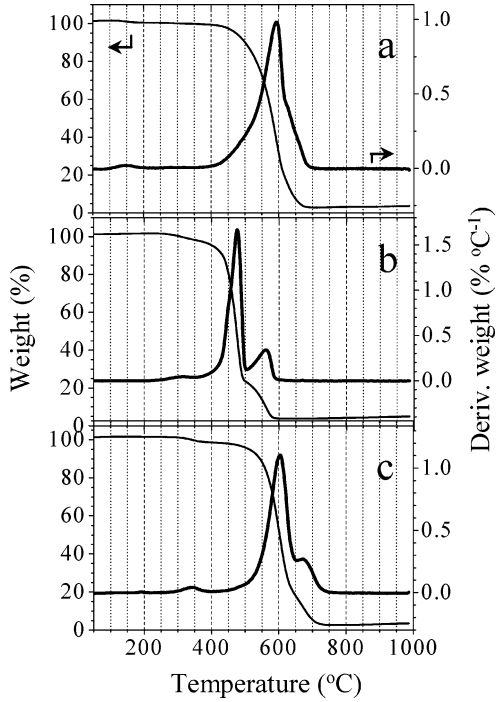

Figure 5. Thermogravimetry (thin lines) and differential thermogravimetry (bold lines) curves of (a) CDDP@NHox immersed in water for 1 day, followed by washing with water and drying, (b) NHox treated with PBS, and (c) NHh treated with PBS.

Reasons for the End of CDDP Release from NHox. The differences between CDDP@NHox and CDDP@NHh in the quantity of the CDDP released in PBS likely stem from the effect of PBS on NHox and NHh. One of the plausible explanations would be that the ions in PBS reacted with the functional groups at the hole edges of NHox, and thus the holes were plugged. The validity of this idea was confirmed by the two experiments shown below.

First, the release medium was changed from PBS to water. It was found that a considerable quantity of CDDP was released. TGA measurements of CDDP@NHox after immersion in water for 1 day indicated that Pt residue at 1000 °C was only about 3 wt % (Figure 5a); that is, about 83% of CDDP was released from inside NHox. This finding differs greatly from that of CDDP release from CDDP@NHox in PBS (Figure 4).

Second, we performed the TGA of PBS−NHh and PBS−NHox. They were prepared by stirring NHh or NHox with PBS, followed by washing with water and drying. The results indicated that the PBS immersion slightly reduced the combustion temperature of NHh from about 635 to 600 °C (Figure 5c), while it greatly reduced that of NHox from 635 to 475 °C (Figure 5b). We ascribe this large decrease for NHox to a chemical instability brought as a result of a chemical reaction of the ions in the PBS with the oxygen-containing groups at the hole edges of the NHox. This is similar to a previous finding that the combustion temperature of NHox is greatly reduced by the chemical modification of the oxygen-containing groups at the hole edges.[22]

We thus conclude that the small quantity of CDDP released from CDDP@NHox in PBS was due to the ions attached to the functional groups at the hole edges, thus plugging the holes. The ions attached to the hole edges of NHox were clarified through the XEDS measurements, which are shown next.

Plug Effect Caused Mainly by −COONa and −ONa Groups. To identify the ions attached to the hole edges, we measured the energy-dispersive X-ray spectra of aggregates of

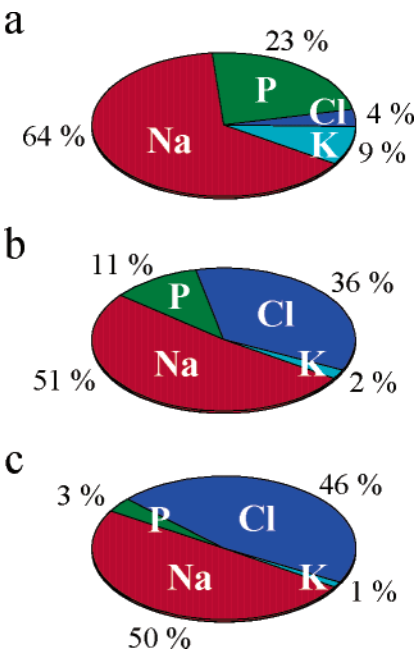

Figure 6. Number ratio of Na/P/Cl/K indicated with a percentage. The circle graphs are for (a) PBS−NHox, (b) PBS−NHh, and (c) PBS.

PBS−NHox and PBS−NHh with a 200-nm probe corresponding to two or three aggregates. We repeated this measurement until 100 aggregates have been probed to obtain average values. The results, shown in Figure 6, indicate that the number ratio of Na/P/Cl/K for PBS−NHh (Na/P/Cl/K = 51:11:36:2, Figure 6b) was close to that for PBS itself (Na/P/Cl/K = 50:3:46:1, Figure 6c), indicating that they existed as NaCl, KCl, and phosphates. However, this number ratio for PBS−NHox was considerably different from that for PBS and indicated that a large amount of Cl was lost (Na/P/Cl/K = 64:23:4:9, Figure 6a). These results suggested that the −COOH and −OH groups at the hole edges changed mainly to −COONa and −ONa groups and hindered the cisplatin release from the NHox. Moreover we found that the quantity of Na absorbed in NHox (number ratio of C/Na = 1000:2.5) corresponds to 24 atoms of Na for a 40-nm-long and 2-nm-wide NHox. If we assume that phosphate formed sodium salt and the remaining sodium reacted at the functional groups at the hole edges, then it is 7 Na atoms per NHox. This value is comparable with the number of possible −ONa and −COONa groups attachable at edge of a hole with a diameter of 1−1.5 nm as we simulate below. We assume that the potassium ions reacted in a similar manner.

We investigated the possibility of the plug effect numerically. Here, the covalent radii of the H (37 pm), O (73 pm), and Na (154 pm), together with the van der Waals radii of the Na (227 pm) and of the H (120 pm), were used for the calculation. The calculation showed that when a hydrogen atom of the −OH group is replaced by Na (that is, formation of the −ONa group) steric hindrance of functional groups increased by 130 pm. As illustrated in Figure 7b, this replacement induces the shrinkage of *effective hole size* from 0.8 nm (orange circle) to 0.6 nm (red circle). We assume that the hole size used here was 1.2 nm according to previous report.[20] Figure 7c showed that the *effective hole sizes* of 0.8 nm (orange circle) shrank to 0.4 nm by −COOH changing to −COONa. Since the molecular size of CDDP is about 0.4 nm × 0.6 nm with a thickness of about 0.1 nm, the CDDP molecules would have trouble passing through the holes with −COONa and −ONa groups attached to the hole edges.

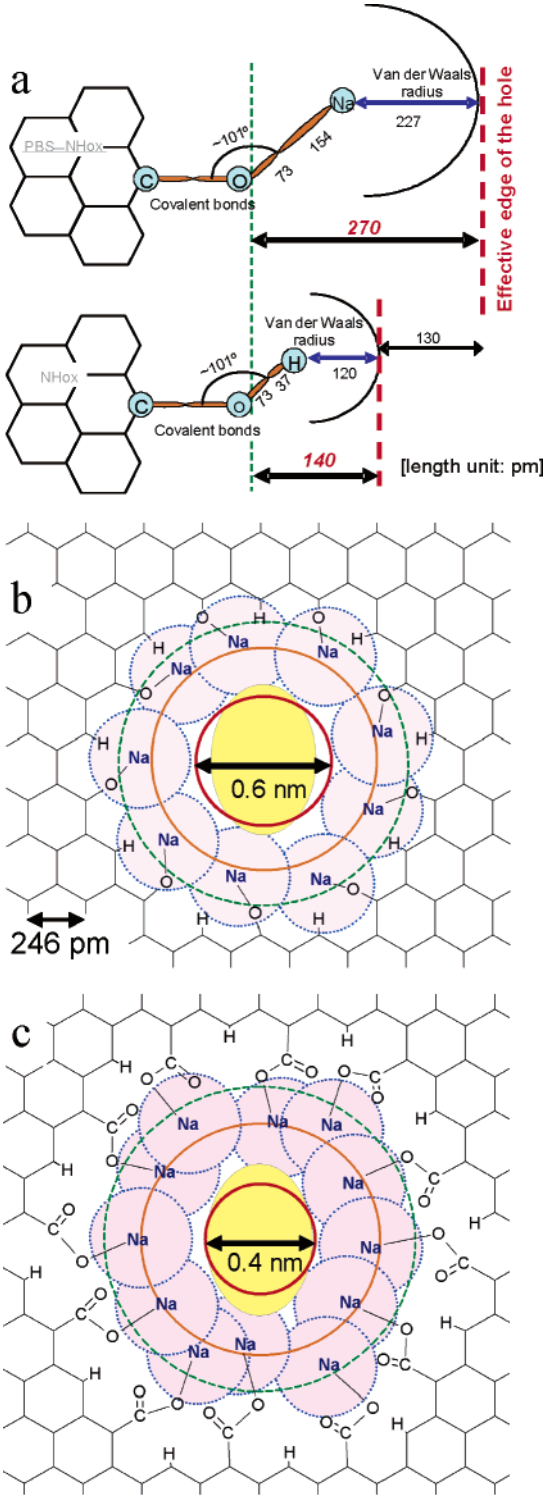

Figure 7. (a) Configurations of −OH and −ONa attached to the hole edges. Models for a hole in a graphene layer having the hole edge modified by (b) −ONa and (c) −COONa groups. The green dashed-line circles (diameters, (b) 1.2 nm or (c) 1.3 nm) represent the hole edges seen in HRTEM observations. Around each Na atom a blue disk (van der Waals radius, 227 pm) has been drawn. No atom can penetrate in this area (except if they are chemically bonded) due to a too high atomic repulsion. The *effective hole size* is determined by these van der Waals areas, which are indicated with red circles (diameters, (b) 0.6 nm or (c) 0.4 nm). In our model (c), the *effective hole size* shrinks down to 0.4 nm, which is too small for a CDDP molecule to pass through (shown in yellow). For comparison, the orange circle (diameters of about 0.8 nm) represents the *effective hole size* with −OH or −COOH groups attached.

Conclusion

Structure analysis of CDDP@NHox and CDDP@NHh indicated that they were similar in the structure, the quantities of incorporated CDDP, and the sizes of CDDP clusters. However, the quantity of CDDP released from CDDP@NHox in PBS was only 15%, while that from CDDP@NHh was 70%. The CDDP release stopping from NHox was due to the plug effect; that is, −COONa and −ONa groups took over the −COOH and −OH groups attached to the hole edges of the NHox and sterically hindered the CDDP passing through the holes from inside NHox. Since NHh had holes with the hydrogen-terminated edges, such a replacement could not happen; thus the plug effect was not observed. These results indicate that the release quantity and rate of the material incorporated inside NHox would be controlled by chemically modifying the functional groups at the hole edges of NHox, which lead to an enhancement of the potential applicability of NHox to the material carriers.

Acknowledgment. We are grateful to Dr. Takeshi Azami and Dr. Daisuke Kasuya of the NEC Corporation for preparing the single-wall carbon nanohorns. A.M. is grateful to the French Ministry of Foreign Affairs for the Lavoisier fellowship.

References and Notes

(1) Matsumura, Y.; Maeda, H. *Cancer Res.* **1986**, *46*, 6387.
(2) Konishi, M.; Tabata, T.; Kariya, M.; Suzuki, A.; Mandai, M.; Nanbu, K.; Takakura, K.; Fujii, S. *J. Controlled Release* **2003**, *92*, 301.
(3) Iga, K.; Hamaguchi, N.; Igari, Y.; Ogawa Y.; Gotoh, K.; Ootsu, K.; Toguchi, H.; Shimamoto, T. *J. Pharmacol. Exp. Ther.* **1991**, *257*, 1203.
(4) Nishiyama, N.; Okazaki, S.; Cabral, H.; Miyamoto, M.; Kato, Y.; Sugiyama, Y.; Nishio, K.; Matsumura, Y.; Kataoka, K. *Cancer Res.* **2003**, *63*, 8977.
(5) Tamura, T.; Fujita, F.; Tanimoto, M.; Koike, M.; Suzuki, A.; Fujita, M.; Horikiri, Y.; Sakamoto, Y.; Suzuki, T.; Yoshino, H. *J. Controlled Release* **2002**, *80*, 295.
(6) Itoi, K.; Tabata, C. Y.; Ike, O.; Shimizu, Y.; Kuwabara, M.; Kyo, M.; Hyon, S. H.; Ikada, Y. *J. Controlled Release* **1996**, *42*, 175.
(7) Idani, H.; Matsuoka, J.; Yasuda, T.; Kobayashi, K.; Tanaka, N. *Int. J. Cancer* **2000**, *88*, 645.
(8) Mizumura, Y.; Matsumura, Y.; Hamaguchi, T.; Nishiyama, N.; Kataoka, K.; Kawaguchi, T.; Hrushesly, W. J. M.; Moriyasu, F.; Kakizoe, T. *Jpn. J. Cancer Res.* **2001**, *92*, 328.
(9) Nishiyama, N.; Yokoyama, M.; Aoyagi, T.; Okano, T.; Sakurai, Y.; Kataoka, K.; *Langmuir* **1999**, *15*, 377.
(10) Wada, R.; Hyon, S. H.; Nakamura, T.; Ikada, Y. *Pharm. Res.* **1991**, *8*, 1292.
(11) Matsumoto, A.; Matsukawa, Y.; Suzuki, T.; Yoshino, H.; Kobayashi, M. *J. Controlled Release* **1997**, *48*, 19.
(12) Iijima, S. *Nature* **1991**, *354*, 56.
(13) Ajayan, P. M.; Iijima, S. *Nature* **1993**, *361*, 333.
(14) Katz, E.; Willner, I. *ChemPhysChem* **2004**, *5*, 1084.
(15) Lin, Y.; Taylor, S.; Li, H.; Fernando, K. A. S.; Qu, L.; Wang, W.; Gu, L.; Zhou, B.; Sun, YP. *J. Mater. Chem.* **2004**, *14*, 527.
(16) Bekyarova, E.; Ni, Y.; Malarkey, E. B.; Montana, V.; McWilliams, J. L.; Haddon, R. C.; Parpura, V. *J. Biomed. Nanotechnol.* **2005**, *1*, 3.
(17) Iijima, S.; Yudasaka, M.; Yamada, R.; Bandow, S.; Suenaga, K.; Kokai, F. Takahashi, K. *Chem. Phys. Lett.* **1999**, *309*, 165.
(18) Murakami, T.; Ajima, K.; Miyawaki, J.; Yudasaka, M.; Iijima, S.; Shiba, K. *Mol. Pharm.* **2004**, *1*, 399.
(19) Ajima, K.; Yudasaka, M.; Murakami, T.; Maigné, A.; Shiba, K.; Iijima, S. *Mol. Pharm.* **2005**, 2, 475.
(20) Ajima, K.; Yudasaka, M.; Suenaga, K.; Kasuya, D.; Azami, T.; Iijima, S. *Adv. Mater.* **2004**, *16*, 397.
(21) Murata, K.; Kaneko, K.; Steele, W. A.; Kokai, F.; Takahashi, K.; Kasuya, D.; Hirahara, K.; Yudasaka, M.; Iijima, S. *J. Phys. Chem. B* **2001**, *105*, 10210.
(22) Miyawaki, J.; Yudasaka, M.; Iijima, S. *J. Phys. Chem. B* **2004**, *108*, 10732.
(23) Yuge, R.; Yudasaka, M.; Miyawaki, J.; Kubo, Y.; Ichihashi, T.; Imai, H.; Nakamura, E.; Isobe, H.; Yorimitsu, H.; Iijima, S. *J. Phys. Chem. B* **2005**, *109*, 17861.
(24) Fan, J.; Yudasaka, M.; Kasuya, D.; Azami, T.; Yuge, R.; Imai, H.; Kubo, Y.; Iijima, S. *J. Phys. Chem. B* **2005**, *109*, 10756.